Title

- Temperature effect on phase state and reactivity controls atmospheric multiphase chemistry and transport of PAHs

Short title

- Phase state controls PAH multiphase chemistry.

One-sentence teaser

Atmospheric refrigerator increases the global transport and health risks of carcinogenic PAHs.

Authors

Q. Mu,[1†] M. Shiraiwa,[1,2] M. Octaviani,[1†] N. Ma,[3,1] A. Ding,[4,5] H. Su,[3,1*] G. Lammel,[1,6*] U. Pöschl,[1] Y. F. Cheng,[1,3*]

Affiliations

1 Multiphase Chemistry Department, Max Planck Institute for Chemistry, P.O. Box 3060, 55128 Mainz, Germany.
2 Department of Chemistry, University of California, Irvine, 92697-2025 California, USA.
3 Institute for Environmental and Climate Research, Jinan University, 511443 Guangzhou, China.
4 Joint International Research Laboratory of Atmospheric and Earth System Sciences, School of Atmospheric Sciences, Nanjing University, 210023, Nanjing, China.
5 Jiangsu Provincial Collaborative Innovation Center of Climate Change, 210023, Nanjing, China.
6 Research Centre for Toxic Compounds in the Environment, Masaryk University, Kamenice 5, 62500 Brno, Czech Republic.
*Corresponding author
† These authors contributed equally to this work.

Abstract

The polycyclic aromatic hydrocarbons like benzo(a)pyrene (BaP) in atmospheric particulate matter pose a threat to human health because of their high carcinogenicity. In the atmosphere, BaP is mainly degraded through the multiphase reaction with ozone, but the fate and atmospheric transport of BaP are poorly characterized. Earlier modeling studies used reaction rate coefficients determined in laboratory experiments at room temperature, which may overestimate/underestimate the degradation rates when applied under atmospheric conditions. Moreover, the effects of diffusion in the particle bulk are not well constrained, leading to large discrepancies between model results and observations. Here we show how the regional and global distributions and transport of BaP can be explained by a new kinetic scheme that provides a realistic description of the temperature and humidity dependence of phase state, diffusivity and reactivity of BaP-containing particles. Low temperature and humidity can substantially increase the lifetime of BaP and enhance its atmospheric dispersion through both the planetary boundary layer and the free troposphere. The new scheme greatly improves the performance of multi-scale models, leading to better agreement with observed BaP concentrations in both source regions and remote regions (Arctic) which cannot be achieved by less elaborate degradation schemes (deviations by multiple orders of magnitude). Our results highlight the importance of considering temperature and humidity effects on both the phase state of aerosol particles and the chemical reactivity of particulate air pollutants.

MAIN TEXT

Introduction

Polycyclic aromatic hydrocarbons (PAHs) are derived from combustion processes. High health risks are associated with exposure to PAHs, among which benzo(a)pyrene (BaP) is one of the most carcinogenic species (*1, 2*). Since BaP resides almost entirely in the particulate phase, the distribution and long-range atmospheric transport of BaP are largely controlled by its multiphase degradation, mainly the reaction of particulate BaP with gaseous ozone (*3*). Laboratory studies showed a fast BaP degradation on the surface of soot, ammonium sulfate and organic aerosol particles (*4–6*), while atmospheric observations revealed much longer lifetime and persistency of BaP especially towards remote and polar regions (*7, 8*). Recent laboratory and kinetic studies have shown that organic aerosol (OA) coatings can effectively shield BaP from oxidants and that the OA phase state may strongly influence the rate of degradation (*9–13*). However, the key factors controlling the multiphase degradation and the fate of BaP in aerosols under real atmosphere conditions are still not resolved (*14*). In particular, the laboratory derived degradation schemes of BaP that have been applied in previous model studies (Fig. 1A, Table S1) (*14–21*) do not fully account for the dependency on environmental conditions/parameters.

Temperature and relative humidity (RH) in the atmosphere cover a wide range, which not only influence the phase state and diffusivity of OA (*12*) but also the chemical reactivity of organic compounds. Since most modeling studies used degradation rates determined at room temperature (i.e., 296–298 K) in laboratory experiments, it may overestimate the degradation rates when applied in colder atmospheric environment. Based on Zhou et al. (*11*), Shrivastava et al. (*14*) introduced a threshold temperature below which the OA coating was assumed to shut off the multiphase degradation of BaP. This shielding effect improved the agreement between model predictions and observations and was very sensitive to the choice of the threshold temperature. A simple threshold value, however, does not resolve the actual temperature dependence of multiphase reactions because both the molecular diffusivity and chemical reactivity of BaP are expected to exhibit a continuous change in response to changing temperature rather than following a step function (*13*).

Moreover, the effects of diffusion and reaction in the particle bulk are not well characterized in earlier studies. For example, most laboratory experiments (*4, 5, 11, 22*) were carried out under excessively high ozone concentrations (up to 3 orders of magnitude above tropospheric levels) and often surface reaction rate equations were used to extrapolate the laboratory results for application in atmospheric models. The use of surface reaction rate equations without considering bulk processes, however, can result in inconsistent dependencies of BaP degradation rates on RH and ozone concentration (Text S1).

In this study, we use an advanced kinetic model framework to develop an elaborate kinetic scheme ROI-T for better representation of multiphase degradation of BaP in regional and global models. This new scheme has incorporated three major improvements compared to previous schemes: (1) considering the formation of reactive oxygen

intermediates (ROI); (2) including the temperature and humidity effects on phase state of OA and temperature-dependent chemical reactivity; and (3) using a model framework that considers both bulk diffusion/reaction and surface reaction to interpret laboratory results for application in models and comparison to field measurements. We find that the new ROI-T scheme can well predict the BaP concentrations from regional to global scales. Our results highlight the importance of temperature on BaP multiphase degradation from a kinetic view and present a universal scheme that can be applied for various atmospheric conditions and geo-locations. Due to the common existence of OA coating, similar temperature effects are expected for other multiphase reactions, which can be determined from laboratory studies by the general modeling framework and approaches proposed here.

Results

BaP degradation kinetic scheme

In the new kinetic scheme ROI-T, the multiphase degradation of BaP with ozone is treated in multiple compartments as shown in Fig. 1B, which has not yet been fully considered by previous schemes. The reaction involves the decomposition of surface ozone and formation of ROI (*23*). To account for the mass transport and reactions of gaseous and particle-bound chemical species at the surface and in the bulk phase, we apply the kinetic multi-layer model of aerosol surface and bulk chemistry (KM-SUB) (*24*, see section M3) which is based on the Pöschl-Rudich-Ammann framework (*25*). Secondary organic aerosol formed from α-pinene oxidation is chosen to represent the OA coating (*11*). With the kinetic parameters in Table S2, the new kinetic scheme ROI-T can well explain the kinetics of multiphase degradation of BaP and successfully reproduce the results of the Zhou's experimental data (*11*) for both thin and thick coating cases (8 nm and 40 nm) at different RH (i.e., dry, 50% and 70%). In further regional/global model applications, the thick coating scenario is adopted, since the global simulation has found that the OA shielding on BaP is generally thick (*14*). As shown in Fig. 1A, rather than a fixed degradation rate, the rate coefficients of the ROI-T scheme show a monotonic increase with increasing temperature and systematically smaller degradation rate of BaP at lower RH.

The temperature- and RH-dependences of diffusivity and BaP chemical reactivity both control the degradation rate of BaP. In the new ROI-T scheme, on the one hand, temperature influences OA diffusivity and its phase state, i.e., the diffusion coefficients of ozone and BaP are assumed to decrease by one order of magnitude upon a decrease of temperature by 10 °C (*26*, see section M3). On the other hand, temperature influences the chemical reactivity of BaP with ROI following the Arrhenius equation (see section M3). Considering both effects, the degradation rates of BaP at 253 K are 3–4 orders of magnitude smaller than those at 313 K (Fig. 1A).

To demonstrate the advantage of the new ROI-T scheme, we have also included other commonly used degradation schemes of BaP: Kwamena (*5*), Kahan (*22*) and Pöschl (*4*) schemes refer to ozonolysis of uncoated BaP on azelaic acid, liquid substrates and soot, respectively; Zhou scheme (*11*) refers to ozonolysis of OA coated BaP. As shown in Fig. 1A, these schemes show different degradation rates due to the substrate and shielding effects as summarized in Table S1.

Model versus observation

Different BaP degradation schemes predict well only on specific characteristic distance from sources or geo-locations, but less on others. For example, the Kwamena scheme shows the best agreement with observations at the mid-latitude, while the optimum scheme for the Arctic is the scheme that predicts the slowest degradation rates, i.e., Kahan scheme (*17, 19*) (Fig. 1A). The ROI-T scheme, on the contrary, is able to account for the different temperature/RH regimes along transport.

In Fig. 2A, we compare the performance of the kinetic ROI-T scheme and the most commonly used Kwamena scheme (*15, 18, 21, 27*) in multi-scale model simulations (see sections M1 and M2). The model results from the Pöschl scheme (the fastest) and the Kahan scheme (the slowest) (Fig. 1A) are also included as references. The observational data used for model evaluation covers a wide range of source/receptor sites over a large span of latitudes (33–83° N, see M4). Compared with other schemes, the ROI-T scheme consistently provides better predictions at all types of sites, from near-source, middle latitude, remote background, to the Arctic (Table S4). It improves the BaP simulation most significantly at the Arctic sites where the arrived air masses undergo the longest and coldest transport processes. For example, the simulated BaP levels at the Alert and Spitsbergen sites are improved by more than one order of magnitude with the ROI-T scheme compared with the Kwamena scheme (Table S4A).

To further elucidate the advantage of the ROI-T scheme, we focus on two cases with contrasting temperature/RH conditions (Fig. 2B): a near-source site Xianghe (39.80° N, 116.96° E, 45 km southeast of Beijing, China) in July representing the local surface transport in hot/humid environment and a remote background site Gosan (33.28º N, 126.17º E, on the Jeju Island, about 100 km south of the Korean peninsula) in February representing long-range transport in cold/dry air. The results show that it is impossible to reproduce observations for both cases by a fixed degradation rate. The Kwamena scheme is either too slow for the Xianghe summer case or too fast for the Gosan winter case, suggesting strong temperature and humidity effects on the diffusivity and reactivity. The model performance cannot be improved by simply changing for another degradation rate, because a higher (lower) degradation rate will reduce (increase) the BaP concentrations at both sites. As shown in Fig. 2A–2B, a scheme with faster degradation rates, such as Pöschl scheme, reduces the BaP concentration to the same level as observations for the Xianghe case but shows a larger underestimation for the Gosan case. We also test the step function setting of the Zhou scheme as in Shrivastava et al. (*14*) It cannot reproduce BaP observations over both cases either, with a very similar performance as the Kahan scheme (the slowest) (Fig. 2B).

By unifying the impact of temperature and RH on diffusivity and reactivity under an elaborate kinetic framework (Fig. 1B), the ROI-T scheme solves the problem with changing BaP degradation rates in response to the changes of environmental conditions (Fig. 1A). Under the new scheme, the hot/humid conditions increase the diffusivity/reactivity and the BaP degradation rate, while it is the other way around in the cold/dry environment. Compared with the Kwamena scheme, our ROI-T scheme leads to reduced BaP concentrations at the Xianghe site and elevated BaP concentration at the Gosan site, finally showing good agreements for both cases. The changes in both diffusivity and chemical reactivity contribute to the changes of degradation rate in the new ROI-T scheme. To decouple their effects, we perform sensitivity studies by turning on/off temperature/RH dependence of diffusivity. At the Gosan site, a fixed degradation rate in

ROI-T scheme at room temperature 296 K leads to an underestimation of BaP concentration by a factor of 3. Further tests show that the temperature/RH induced change of diffusivity would account for ~ 50% of the improvement in the predicted BaP concentrations while the change of reactivity further contributes to the rest of the ~ 50% (as shown by the comparison between "ROI-T at 296 K" and "ROI-T with fixed diffusivity" cases in Fig. S1).

East Asia outflow

As one of the largest source regions, the outflow of BaP from East Asia to the downwind regions and remote Pacific Ocean is of international concern (*28, 29*). Figure 3A and 3B show a typical outflow transport of BaP from East Asia in winter (24 February 2003). With the Kwamena scheme, most BaP is bounded in the boundary layer due to fast degradation with an average lifetime of ~ 2 to 3 hours throughout the whole domain (Fig. S2), resulting in very low concentrations above 1 km (Fig. 3A). The decrease of degradation rate resulting from the change in temperature and RH during air mass rising (see temperature and RH distribution in Fig. S3) is, however, not accounted for. Even when BaP is able to escape out of the boundary layer by large-scale advections associated with cyclones or by convections in mid-latitudes (i.e. 35–45° N), fast degradation limits dispersion and transport of BaP to the vicinity of the source region. Thus, the transport of BaP with the Kwamena scheme is constrained within the boundary layer and the long-range transport impacts are limited.

The ROI-T scheme shows a different spatial distribution and transport pathway of BaP, with more BaP distributed at higher altitude. This is because low temperature reduces OA diffusivity and reaction rate of BaP with ROI ("freezing effect", see 3-D degradation rate *k* in Fig. S2) and thus leads to a much longer lifetime of BaP above 1 km (~ 2 to 3 hours to more than 20 days, Fig. S2), making transport in the free troposphere an efficient pathway. Compared with the Kwamena scheme, 15 times more BaP is lifted by frontal activities and convection to middle-troposphere, where strong westerlies/jets cause a fast transport of the plumes to downwind areas (Fig. S5–S6 and Text S2) and towards polar region, resulting in much stronger global impacts. At the cross section of 126° E (Fig. 3A–3B), the BaP outflow towards the ocean shows a maximum zonal net flux of ~ 35 ng m^{-2} s^{-1} in the ROI-T scheme but only ~ 10 ng m^{-2} s^{-1} in the Kwamena scheme (Fig. S4A-S4B). It is also clear that the vertical center of the BaP column mass in the ROI-T scheme is higher than that in the Kwamena scheme, i.e., ~ 0.6 km and 0.3 km, respectively (Fig. S4C-S4D).

Transport to the Arctic

BaP emitted in source regions can undergo intercontinental transport, allowing them to distribute and accumulate even in the polar regions (*7, 30*). The concentration level of BaP in the Arctic arouses high interest, because BaP is not only a good indicator of human contamination (*30*), but also responsible for the severe bioconcentrate effect in the Arctic (*31*) where the ecosystem is most vulnerable, bioaccumulation along marine and terrestrial food chains (*31–33*). As shown in the East Asia outflow case, the "freezing effect" may make the intercontinental transport of BaP from source regions to the Arctic at high altitude or low temperature region more efficient than previously thought.

As shown in Fig. 3C–D, BaP in the Arctic is mainly transported from Europe, North America and Asia, similar to long-lived halogenated pollutants (*34*). The 2007–2009 average total meridional net flux of BaP towards the Arctic (integrated over 1000–10 hPa at 65° N) is 1.97 ng m^{-2} s^{-1} with the ROI-T scheme, but only 0.12 ng m^{-2} s^{-1} with the Kwamena scheme (Fig. S4E), which is about 16 times lower. The larger fluxes of BaP with the ROI-T scheme can be attributed to a longer lifetime of BaP caused by the "freezing effect" (Fig. S2), as the pollutant is transported significantly higher. The average vertical center of the BaP column mass transported across 65° N during 2007–2009 is 2 km for the ROI-T scheme but only 0.5 km for the Kwamena scheme. (Fig. S4F), showing a difference in height more prominent than in the East Asian outflow case.

Discussion

The strong temperature/RH effects on fate and global transport of BaP advance the understanding and challenge the traditional view of modeling the multiphase degradation of reactive pollutants (e.g., BaP) in organic aerosols. In warm/humid environments (e.g., tropical rainforests), aerosol particles tend to be liquid, while in cold environments, aerosols are found to be in an amorphous solid phase, most probably glassy state (*12*). The phase state and degradation rate of BaP may vary largely depending on temperature/RH and hence the season (summer vs winter), altitude (surface vs high altitude) and latitude (tropical vs polar) (Fig. 4). It also emphasizes the importance of higher altitude or cold season/region pathway for the long-range transport, i.e., the low temperature helps OA and reactive compounds within it survive from the multiphase chemistry, remaining un-degraded and being transported further.

The ROI-T scheme is based on the kinetic data observed on the ozonolysis of BaP coated by α-pinene SOA. Recent studies have suggested that α-pinene SOA is less viscous than aromatic SOA and is more viscous than isoprene SOA (*35, 36*). SOA particles are also often internally mixed with inorganic components, which may affect particle phase state, non-ideal mixing and morphology and hence the multiphase reaction rates (*37*). Therefore, the effects of different SOA precursors and inorganic interactions should be further explored. Partitioning of PAHs to other organic aerosols such as bioparticles is less efficient than to liquid and semi-solid SOA (*38*). The presence of more viscous bioparticles will lead to less reactive PAHs and therefore an even higher long-range transport potential.

The large impact of temperature/RH on the diffusivity/reactivity is not limited to the degradation of BaP but has general implications for all kinds of multiphase reactions in aerosols, clouds and fog droplets relevant for atmospheric chemistry and transport (*9,12,39,40*). The impact is particularly important for the northern hemisphere where efficient large-scale advection/convection associated with cyclones and strongest anthropogenic emissions exist. Our results demonstrate that it is important to perform laboratory kinetic studies on the large temperature/RH span relevant for atmospheric conditions. Our modeling scheme provides an advanced physicochemical based framework for the representation of multiphase reaction in atmospheric models and can be readily modified to include other hazardous air pollutants and OA species once the kinetic data are available.

Materials and Methods

M1. Model Setup

The ROI-T scheme is incorporated as a look-up table (Table S3) into two state-of-the-art models with BaP extension for further application.

Regional model

The open source community model WRF-Chem (Weather Research and Forecasting model coupled with Chemistry), an "online" regional model with coupled meteorology and chemistry (*41,42*), has higher spatial resolution and advantages in determining the fine structures of transport process, especially the vertical transport within and out of the boundary layer. The PAH extension is based on the model version 3.6.1.

The physics schemes of the regional WRF-Chem model used here are as follows (*42*): microphysics and cumulus parameterizations follow the Purdue–Lin scheme and the Grell 3D ensemble scheme, respectively. The longwave and shortwave radiation are calculated by the online rapid radiative transfer model and the Goddard scheme, respectively. The planetary boundary layer is based on the Mellor–Yamada–Janjic scheme, along with the Eta Similarity surface layer scheme. The implemented air-soil gas exchange is coupled with the Noah Land Surface Model. Photolysis rates use the Fast-J photolysis scheme. As for the chemistry schemes, the Regional Atmospheric Chemistry Mechanism (RACM) is used for homogeneous gas-phase reactions. The aerosol module includes the inorganic fraction Modal Aerosol Dynamics Model for Europe (MADE) and organic fraction Secondary Organic Aerosol Model (SORGAM).

Global model

The global model EMAC (ECHAM/MESSy Atmospheric Chemistry) covers intercontinental transport, such as from source areas to the Arctic. It is a combination of the ECHAM5 general circulation model (*43*) and MESSy (Modular Earth Submodel System, version 2.5) (*44*). MESSy provides infrastructure to couple the base model ECHAM5 and different components (or submodels) that represent various processes of the Earth system.

The model simulations include the following MESSy submodels (*44*): CLOUD describes cloud scheme and precipitation. Convection parameterization and radiation are in submodels CONVECT and RAD. Air-sea exchange is parameterized by AIRSEA. Wet and dry depositions are described by SCAV and DDEP. Prescribed emissions are calculated by OFFLEM while online emissions by ONLEM. As for chemistry, MECCA is responsible for gas-phase chemistry, JVAL takes care of photolysis rate, and GMXe is the submodel for aerosol microphysics and semi-volatile inorganic partitioning.

Simulation

We perform regional (global) simulations at a grid spacing of 27 km × 27 km (1.9° × 2.5°) with 39 (19) vertical levels from the surface to 100 hPa (10 hPa). Simulations are conducted during 11–22 July 2013 for Xianghe case and 14–25 February 2003 for Gosan case over East Asia domain (15–55º N, 95–155º E) by the regional model, and 2007–2009 for mid-latitude and Arctic sites by the global model, respectively.

M2. BaP extension

The following processes of BaP are included: emission, gas-particle partitioning, gas phase and multiphase reactions, air-soil gas exchange, wet and dry depositions.

Emissions

Anthropogenic BaP emissions are re-gridded from a 0.1° × 0.1° global annual PAH emission inventory, with 69 detailed source types (*45*). Monthly variation is based on BC emission seasonality of HTAP_v2.2 (*46*). For regional simulations, annual scaling factors

(*45*) and diurnal cycle (following BC) of the PAH emissions are also applied. Biogenic contributions to PAH emission have been neglected.

Gas−particle partitioning

Gas−particle partitioning of BaP used in the regional model follows an equilibrium partitioning expression which accounts for absorption into organic matter and adsorption onto black carbon (*47,48*). In the global model, polyparameter linear free energy relationships are applied which account for BaP absorption into organic matter and adsorption to soot and inorganic salts (*38*).

Gas-phase reaction

The second-order rate coefficients for reactions of gaseous BaP with OH, NO_3, and O_3 are 1.5×10^{-10}, 5.4×10^{-11} and 2.6×10^{-17} cm^3 $molec^{-1}$ s^{-1}, respectively (*49*).

Wet/dry depositions

The original regional/global model routines have been adapted to include the deposition of gas-phase and particulate-phase BaP using corresponding deposition parameterizations.

Air-soil gas exchange

Air-soil gas exchange of BaP is parameterized (*50*) based on air/soil concentrations and properties of BaP. The concentrations of BaP in soil are initialized by the global multicompartmental model ECHAM5-HAM: BaP has been simulated globally over 10 years with 2.8° x 2.8° horizontal resolution (*51*). A steady state of BaP concentrations in the soil compartment is safely reached.

M3. KM-SUB model

The kinetic multi-layer model of aerosol surface and bulk chemistry (KM-SUB) treats mass transport and chemical reactions at the surface and in the particle bulk (*24*). KM-SUB is composed of the following compartments: gas phase, near-surface gas phase, sorption layer, quasi-static surface layer, near-surface bulk layer, and a number of bulk layers. The model resolves the following processes explicitly: gas-phase diffusion, reversible adsorption of O_3, surface reaction involving decomposition of O_3 and formation of long-lived reactive oxygen intermediates (ROI), bulk diffusion of O_3 and BaP in OA coating, and bulk reaction between O_3 and BaP. Note that heat transfer is not treated in the model as heat released by trace gas uptake and reactions can be efficiently buffered by the ambient gas and does not lead to a substantial increase of particle surface temperature (*52*). KM-SUB can simulate the evolution of species at the particle surface and in the particle bulk, along with surface concentrations and gas uptake coefficients. Core-shell morphology is assumed with an organic phase embedding BaP as particle shell and an inorganic phase as particle core (*37*). The required kinetic parameters are summarized in Table S2 and the values are based on previous studies of KM-SUB applications to experimental data of Zhou et al. (*11*).

The ROI-T considers the temperature dependence of bulk diffusivity and chemical reactivity. The diffusion coefficients of ozone and PAH are assumed to decrease by one order of magnitude upon a decrease of temperature by 10 °C based on the Vogel-Fulcher-Tamman approach (*26, 35*). Temperature-dependence of rate coefficients *k* is considered by the Arrhenius equation using the activation energies of surface reactions as listed in Table S2. KM-SUB simulations are conducted in the temperature range of -20 – 40 °C with gas-phase ozone concentrations of 0 – 200 ppbv. The obtained first-order decay rate of PAH is then fitted with the Hill equation as shown in Table S3, so that the parameterizations can be efficiently incorporated in regional and global transport models.

M4. Observational data of BaP

The near-source observation data of BaP was collected at the Xianghe Atmospheric Observatory (39.80° N, 116.96° E). The Xianghe site is a sub-urban site locating 45 km southeast of Beijing and 70 km northwest of Tianjin. Particulate- and gas-phase samples were collected for daytime (8:00 – 18:00 local time) and nighttime (20:00 – 6:00 local time) respectively during 11–22 July 2013.

The out-flow observation data of BaP was measured at the Gosan site (33.28º N, 126.17º E) on the Jeju Island. The site was 72 m above sea level and about 100 km south of the Korean peninsula. Gosan is a representative background station in East Asia to study out-flow of air pollutants from land to ocean. Intensive daily measurements (8:00–8:00 local time in the following morning) of particulate phase BaP were carried out during a pollution period 14–25 February 2003. Details of sampling and analysis methods are given in Kim et al. (*53*).

The mid-latitude observation data of BaP is taken from 18 stations of the European Monitoring and Evaluation Programme (EMEP) (*54*), the Integrated Atmospheric Deposition Network (IADN) (*55*) and Arctic Monitoring and Assessment Programme (AMAP) (*56*). Three Arctic sites (i.e., north of 66.5° N) are: Alert in Canada (AMAP, 62.3° W, 82.5° N), Spitsbergen in Norway (EMEP, 11.9° E, 78.9° N) and Pallas in Finland (EMEP, 24.3° E, 68.0° N). The concentration of BaP during 2007–2009 is averaged over all months, with at least 1 weekly measurement reported.

H2: Supplementary Materials

Text S1. Problems without considering bulk processes.

Text S2. Warm conveyor belts (WCBs) and BaP transport in Gosan winter case.

Table S1. Flow tube experiments of multiphase degradation of BaP with ozone.

Table S2. Kinetic parameters used in the KM-SUB simulation for the ozonolysis of BaP in order to reproduce experiment results of the Zhou scheme.

Table S3. Parameterization of multiphase degradation rate for the ozonolysis of BaP.

Table S4. Comparisons of observed and predicted BaP concentrations in the regional WRF-Chem model and the global EMAC model.

Fig. S1. Same as Fig. 2B but with 3 more sensitivity studies.

Fig. S2. Multiphase degradation rate and chemical life time.

Fig. S3. BaP concentrations and multiphase degradation rate.

Fig. S4. Net meridional mass flux and vertical center of column mass for BaP in different cases.

Fig. S5. BaP transport due to warm conveyor belt and frontal activities associated with mid-latitude cyclones for the Gosan winter case.

Fig. S6. A conceptual scheme of for air pollution transport due to middle-latitude cyclone.

References (*57–60*)

References and Notes

1 F.P. Perera, Environment and cancer: Who are susceptible? *Science* **278**, 1068–1073 (1997).

2 P. Boffetta, N. Jourenkova, P. Gustavsson, Cancer risk from occupational and environmental exposure to polycyclic aromatic hydrocarbons. *Cancer Cause Control* **8**, 444–472 (1997).

3 I. J. Keyte, R. M. Harrison, G. Lammel, Chemical reactivity and long-range transport potential of polycyclic aromatic hydrocarbons - a review. *Chem. Soc. Rev.* **42**, 9333–9391 (2013).

4 U. Pöschl, T. Letzel, C. Schauer, R. Niessner, Interaction of ozone and water vapor with spark discharge soot aerosol particles coated with benzo[a]pyrene: O_3 and H_2O adsorption, benzo[a]pyrene degradation, and atmospheric implications. *J. Phys. Chem. A* **105**, 4029–4041 (2001).

5 N. O. A. Kwamena, J. A. Thornton, J. P. D. Abbatt, Kinetics of surface-bound benzo[a]pyrene and ozone on solid organic and salt aerosols. *J. Phys. Chem. A* **108**, 11626–11634 (2004).

6 S. Zhou, A. K. Y. Lee, R. D. McWhinney, J. P. D. Abbatt, Burial effects of organic coatings on the heterogeneous reactivity of particle-borne benzo[a]pyrene (BaP) toward ozone. *J. Phys. Chem. A* **116**, 7050–7056 (2012).

7 C. J. Halsall, L. A. Barrie, P. Fellin, D. C. G. Muir, F. Y. Rovinski, *et al.*, Spatial and temporal variation of polycyclic aromatic hydrocarbons in the Arctic atmosphere. *Environ. Sci. Technol.* **31**, 3593–3599 (1997).

8 C. Schauer, R. Niessner, U. Pöschl, Polycyclic aromatic hydrocarbons in urban air particulate matter: Decadal and seasonal trends, chemical degradation, and sampling artifacts. *Environ. Sci. Technol.* **37**, 2861–2868 (2003).

9 M. Shiraiwa, M. Ammann, T. Koop, U. Pöschl, Gas uptake and chemical aging of semisolid organic aerosol particles. *Proc. Natl. Acad. Sci. U. S. A.* **108**, 11003–11008 (2011).

10 T. Berkemeier, S. S. Steimer, U. K. Krieger, T. Peter, U. Pöschl, *et al.*, Ozone uptake on glassy, semi-solid and liquid organic matter and the role of reactive oxygen intermediates in atmospheric aerosol chemistry. *Phys. Chem. Chem. Phys.* **18**, 12662–12674 (2016).

11 S. Zhou, M. Shiraiwa, R. D. McWhinney, U. Pöschl, J. P. D. Abbatt, Kinetic limitations in gas-particle reactions arising from slow diffusion in secondary organic aerosol. *Faraday Discuss.* **165**, 391–406 (2013).

12 M. Shiraiwa, Y. Li, A. P. Tsimpidi, V. A. Karydis, T. Berkemeier, *et al.*, Global distribution of particle phase state in atmospheric secondary organic aerosols. *Nat. Commun.* **8**, 15002 (2017).

13 T. Koop, J. Bookhold, M. Shiraiwa, U. Pöschl, Glass transition and phase state of organic compounds: dependency on molecular properties and implications for secondary organic aerosols in the atmosphere. *Phys. Chem. Chem. Phys.* **13**, 19238–19255 (2011).

14 M. Shrivastava, S. Lou, A. Zelenyuk, R. C. Easter, R. A. Corley, *et al.*, Global long-range transport and lung cancer risk from polycyclic aromatic hydrocarbons shielded by coatings of organic aerosol. *Proc. Natl. Acad. Sci. U. S. A.* **114**, 1246–1251 (2017).

15 V. Matthias, A. Aulinger, M. Quante, CMAQ simulations of the benzo(a)pyrene distribution over Europe for 2000 and 2001. *Atmos. Environ.* **43**, 4078–4086 (2009).

16 A. Aulinger, V. Matthias, M. Quante, An Approach to Temporally Disaggregate Benzo(a)pyrene Emissions and Their Application to a 3D Eulerian Atmospheric Chemistry Transport Model. *Water Air Soil Poll.* **216**, 643–655 (2011).

17 C. L. Friedman, N. E. Selin, Long-range atmospheric transport of polycyclic aromatic hydrocarbons: A global 3-D model analysis including evaluation of Arctic sources. *Environ. Sci. Technol.* **46**, 9501–9510 (2012).
18 R. San Jose, J. L. Perez, M. S. Callen, J. M. Lopez, A. Mastral, BaP (PAH) air quality modelling exercise over Zaragoza (Spain) using an adapted version of WRF-CMAQ model. *Environ. Pollut.* **183**, 151–158 (2013).
19 C. L. Friedman, J. R. Pierce, N. E. Selin, Assessing the influence of secondary organic versus primary carbonaceous aerosols on long-range atmospheric polycyclic aromatic hydrocarbon transport. *Environ. Sci. Technol.* **48**, 3293–3302 (2014).
20 C. L. Friedman, Y. Zhang, N. E. Selin, Climate change and emissions impacts on atmospheric PAH transport to the Arctic. *Environ. Sci. Technol.* **48**, 429–437 (2014).
21 C. I. Efstathiou, J. Matejovičová, J. Bieser, G. Lammel, Evaluation of gas-particle partitioning in a regional air quality model for organic pollutants. *Atmos. Chem. Phys.* **16**, 15327–15345 (2016).
22 T. F. Kahan, N. O. A. Kwamena, D. J. Donaldson, Heterogeneous ozonation kinetics of polycyclic aromatic hydrocarbons on organic films. *Atmos. Environ.* **40**, 3448–3459 (2006).
23 M. Shiraiwa, Y. Sosedova, A. Rouviere, H. Yang, Y. Zhang, *et al.*, The role of long-lived reactive oxygen intermediates in the reaction of ozone with aerosol particles, *Nat. Chem.* **3**, 291–295 (2011).
24 M. Shiraiwa, C. Pfrang, U. Pöschl, Kinetic multi-layer model of aerosol surface and bulk chemistry (KM-SUB): the influence of interfacial transport and bulk diffusion on the oxidation of oleic acid by ozone. *Atmos. Chem. Phys.* **10**, 3673–3691 (2010).
25 U. Pöschl, Y. Rudich, M. Ammann, Kinetic model framework for aerosol and cloud surface chemistry and gas-particle interactions - Part 1: General equations, parameters, and terminology. *Atmos. Chem. Phys.* **7**, 5989–6023 (2007).
26 A. M. Arangio, J. H. Slade, T. Berkemeier, U. Pöschl, D. A. Knopf, *et al.*, Multiphase chemical kinetics of OH radical uptake by molecular organic markers of biomass burning aerosols: Humidity and temperature dependence, surface reaction, and bulk diffusion. *J. Phys. Chem. A* **119**, 4533–4544 (2015).
27 A. Aulinger, V. Matthias, M. Quante, Introducing a partitioning mechanism for PAHs into the Community Multiscale Air Quality modeling system and its application to simulating the transport of benzo(a) pyrene over Europe. *J. Appl. Meteorol. Clim.* **46**, 1718–1730 (2007).
28 Y. Zhang, S. Tao, J. Ma, S. Simonich, Transpacific transport of benzo[a]pyrene emitted from Asia. *Atmos. Chem. Phys.* **11**, 11993–12006 (2011).
29 Y. Zhang, H. Shen, S. Tao, J. Ma, Modeling the atmospheric transport and outflow of polycyclic aromatic hydrocarbons emitted from China. *Atmos. Environ.* **45**, 2820–2827 (2011).
30 V. Hoyau, J. L. Jaffrezo, P. Garrigues, M. P. Clain, P. Masclet, Deposition of aerosols in polar regions-contamination of the ice sheet by polycyclic aromatic hydrocarbons. *Polycycl. Aromat. Comp.* **8**, 35–44 (1996).
31 R. W. Macdonald, J. M. Bewers, Contaminants in the arctic marine environment: Priorities for protection. *Ices J. Mar. Sci.* **53**, 537–563 (1996).
32 R. K. Achazi, C. A. M. Van Gestel, *PAHs: An Ecotoxicological Perspective* (Wiley, New York, 2003)
33 J. P. Meador, J. E. Stein, W. L. Reichert, U. Varanasi, Bioaccumulation of polycyclic aromatic hydrocarbons by marine organisms. *Rev. Environ. Contam. Toxicol.* **143**, 79–165 (1995).

34 M. Octaviani, I. Stemmler, G. Lammel, H. F. Graf, Atmospheric transport of persistent organic pollutants to and from the Arctic under present-day and future climate. *Environ. Sci. Technol.* **49**, 3593–3602 (2015).
35 T. Berkemeier, M. Shiraiwa, U. Pöschl, T. Koop, Competition between water uptake and ice nucleation by glassy organic aerosol particles. *Atmos. Chem. Phys.* **14**, 12513–12531 (2014).
36 M. Song, P. F. Liu, S. J. Hanna, Y. J. Li, S. T. Martin, *et al.*, Relative humidity-dependent viscosities of isoprene-derived secondary organic material and atmospheric implications for isoprene-dominant forests. *Atmos. Chem. Phys.* **15**, 5145–5159 (2015).
37 M. Shiraiwa, A. Zuend, A. K. Bertram, J. H. Seinfeld, Gas-particle partitioning of atmospheric aerosols: interplay of physical state, non-ideal mixing and morphology. *Phys. Chem. Chem. Phys.* **15**, 11441–11453 (2013).
38 P. Shahpoury, G. Lammel, A. Albinet, A. Sofuoğlu, Y. Dumanoğlu, *et al.,* Evaluation of a conceptual model for gas-particle partitioning of polycyclic aromatic hydrocarbons using polyparameter linear free energy relationships. *Environ. Sci. Technol.* **50**, 12312–12319 (2016).
39 Y. F. Cheng, H. Su, T. Koop, E. Mikhailov, U. Pöschl, Size dependence of phase transitions in aerosol nanoparticles. *Nat. Commun.* **6**, 5923 (2015).
40 Y. F. Cheng, G. J. Zheng, C. Wei, Q. Mu, B. Zheng, *et al.*, Reactive nitrogen chemistry in aerosol water as a source of sulfate during haze events in China. *Sci. Adv.* **2**, e1601530 (2016).
41 G. A. Grell, S. E. Peckham, R. Schmitz, S. A. McKeen, G. Frost, *et al.*, Fully coupled "online" chemistry within the WRF model. *Atmos. Environ.* **39**, 6957–6975 (2005).
42 *WRF-Chem Version 3.6.1 User's Guide* (National Center for Atmospheric Research, Boulder, USA, 2014)
43 E. Roeckner, G. Bäuml, L. Bonaventura, R. Brokopf, M. Esch, *et al.*, *The atmospheric general circulation model ECHAM 5. Part I: Model description (MPI-Report No. 349)* (Max Planck Institute for Meteorology, Hamburg, Germany, 2003).
44 P. Jöckel, A. Kerkweg, A. Pozzer, R. Sander, H. Tost, *et al.*, Development cycle 2 of the Modular Earth Submodel System (MESSy2). *Geosci. Model Dev.* **3**, 717–752 (2010).
45 H. Shen, Y. Huang, R. Wang, D. Zhu, W. Li, *et al.*, Global atmospheric emissions of polycyclic aromatic hydrocarbons from 1960 to 2008 and future predictions. *Environ. Sci. Technol.* **47**, 6415–6424 (2013).
46 G. Janssens-Maenhout, M. Crippa, D. Guizzardi, F. Dentener, M. Muntean, *et al.*, HTAP_v2.2: a mosaic of regional and global emission grid maps for 2008 and 2010 to study hemispheric transport of air pollution. *Atmos. Chem. Phys.* **15**, 11411–11432 (2015).
47 R. Lohmann, G. Lammel, Adsorptive and absorptive contributions to the gas-particle partitioning of polycyclic aromatic hydrocarbons: State of knowledge and recommended parametrization for modeling. *Environ. Sci. Technol.* **38**, 3793–3803 (2004).
48 E. Galarneau, P. A. Makar, Q. Zheng, J. Narayan, J. Zhang, *et al.*, PAH concentrations simulated with the AURAMS-PAH chemical transport model over Canada and the USA. *Atmos. Chem. Phys.* **14**, 4065–4077 (2014).
49 W. Klöpffer, B. O. Wagner, K. G. Steinhäuser, Atmospheric degradation of organic substances: Persistence, transport potential, spatial range (Wiley, New York, 2008).
50 W. A, Jury, W. F. Spencer, W. J. Farmer, Behavior assessment model for trace organics in soil .1. Model Description. *J. Environ. Qual.* **12**, 558–564 (1983).
51 G. Lammel, A. M. Sehili, T. C. Bond, J. Feichter, H. Grassl, Gas/particle partitioning and global distribution of polycyclic aromatic hydrocarbons - A modelling approach. *Chemosphere* **76**, 98–106 (2009).

52 M. Shiraiwa, C. Pfrang, T. Koop, U. Pöschl, Kinetic multi-layer model of gas-particle interactions in aerosols and clouds (KM-GAP): linking condensation, evaporation and chemical reactions of organics, oxidants and water. *Atmos. Chem. Phys*. **12**, 2777–2794 (2012).
53 J. Y. Kim, J. Y. Lee, S. D. Choi, Y. P. Kim, Y. S. Ghim, Gaseous and particulate polycyclic aromatic hydrocarbons at the Gosan background site in East Asia. *Atmos. Environ.* **49**, 311–319 (2012).
54 K. Tørseth, W. Aas, K. Breivik, A. M. Fjæraa, M. Fiebig, *et al.*, Introduction to the European Monitoring and Evaluation Programme (EMEP) and observed atmospheric composition change during 1972–2009. *Atmos. Chem. Phys.* **12**, 5447–5481 (2012).
55 E. Galarneau, T. F. Bidleman, P. Blanchard, Seasonality and interspecies differences in particle/gas partitioning of PAHs observed by the Integrated Atmospheric Deposition Network (IADN). *Atmos. Environ.* **40**, 182–197 (2006).
56 H. Hung, R. Kallenborn, K, Breivik, Y. Su, E. Brorström Lundén, *et al.*, Atmospheric monitoring of organic pollutants in the Arctic under the Arctic Monitoring and Assessment Programme (AMAP): 1993–2006. *Sci. Total. Environ.* **408**, 2854–2873 (2010).
57 A. Ding, X. Huang, C. Fu, Air pollution and weather interaction in East Asia. *Oxford Research Encyclopedia of Environmental Science,* DOI:10.1093/acrefore/9780199389414.013.536 (2017).
58 A. Ding, T. Wang, L. Xue, J. Gao, A. Stohl, *et al.*, Transport of north China air pollution by midlatitude cyclones: Case study of aircraft measurements in summer 2007, *J. Geophys. Res.* **114**, D11399 (2009).
59 A. Stohl, Z. Klimont, S. Eckhardt, K. Kupiainen, V. P. Shevchenko, *et al.*, Black carbon in the Arctic: the underestimated role of gas flaring and residential combustion emissions. *Atmos. Chem. Phys.* **13**, 8833–8855 (2013).
60 P. Winiger, A. Andersson, S. Eckhardt, A. Stohl, O. Gustafsson, The sources of atmospheric black carbon at a European gateway to the Arctic. *Nat. Commun.* **7**, 12776 (2016).

Acknowledgments

We would like to thank Qiang Zhang, Yuxuan Zhang and Guangjie Zheng (Tsinghua University, China) for sampling, and Petra Příbylová and Ondřej Audy (Masaryk University, Czech Republic) for chemical analysis at the Xianghe site. We also acknowledge the kind share of BaP concentration data at the Gosan site by Young-Sung Ghim (Hankuk University of Foreign Studies, Korea). **Funding:** We would like to acknowledge the National Natural Science Foundation of China (91644218, 41330635), U.S. National Science Foundation (AGS-1654104), U.S. Department of Energy (DE-SC0018349) and Czech Science Foundation (P503 16-11537S). This work was supported by the Max Planck Society (MPG). Y. C. would also like to thank the Minerva Program of MPG. **Author contributions:** Y.C., H.S., U.P. and G.L. conceived the study. M.S., Y.C., H.S. and U.P. developed the temperature dependent ROI-T scheme for model implementation. Q.M. incorporated new PAH module into the regional model WRF-Chem and performed the model simulation and data analyses. M.O. incorporated new PAH module into the global model EMAC and performed the model simulation and data analyses. Y.C., H.S. and Q.M. analyzed and interpreted results. N.M. contributed to data analysis and visualization. A. D. contributed to the transport process analysis and relevant discussion in the SI. All coauthors discussed the results. H.S., Y.C. and Q.M. wrote the manuscript with input from all coauthors. **Competing Interests**: The authors declare that they have no competing interests. **Data and**

materials availability: All data needed to evaluate the conclusions in the paper are present in the paper and/or the Supplementary Materials. Additional data available from authors upon request.

Figures and Tables

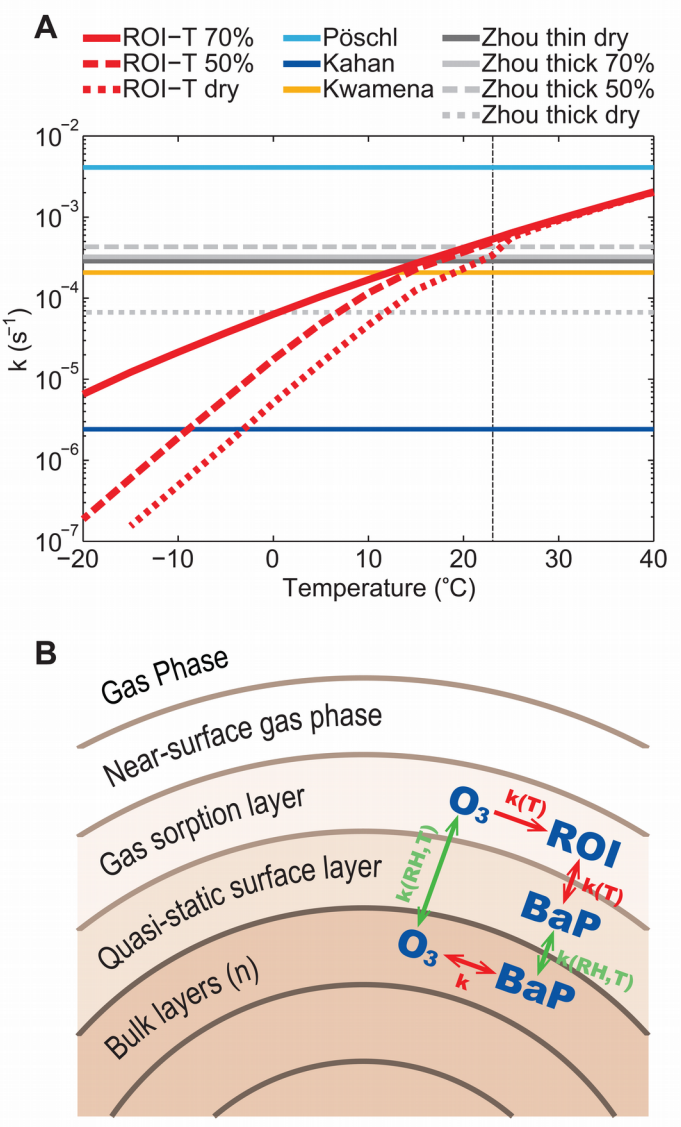

Fig. 1. Kinetic scheme ROI-T. (**A**) First-order multiphase degradation rate coefficient k (s^{-1}) for laboratory schemes Pöschl (*4*), Kahan (*22*), Kwamena (*5*), Zhou (*11*) (Table S1) and the kinetic scheme ROI-T at 50 ppbv O_3. Vertical dashed line denotes 23 ºC. (**B**) Model framework of the multi-layer kinetic scheme ROI-T. Red arrows show the reactions: O_3 is decomposed and forms ROI in the gas sorption layer, BaP reacts with ROI between gas sorption and surface layer, and BaP reacts with O_3 in the bulk. Green arrows show the RH/T-dependent mass transport: O_3 from gas sorption to bulk layer, BaP from bulk to surface layer.

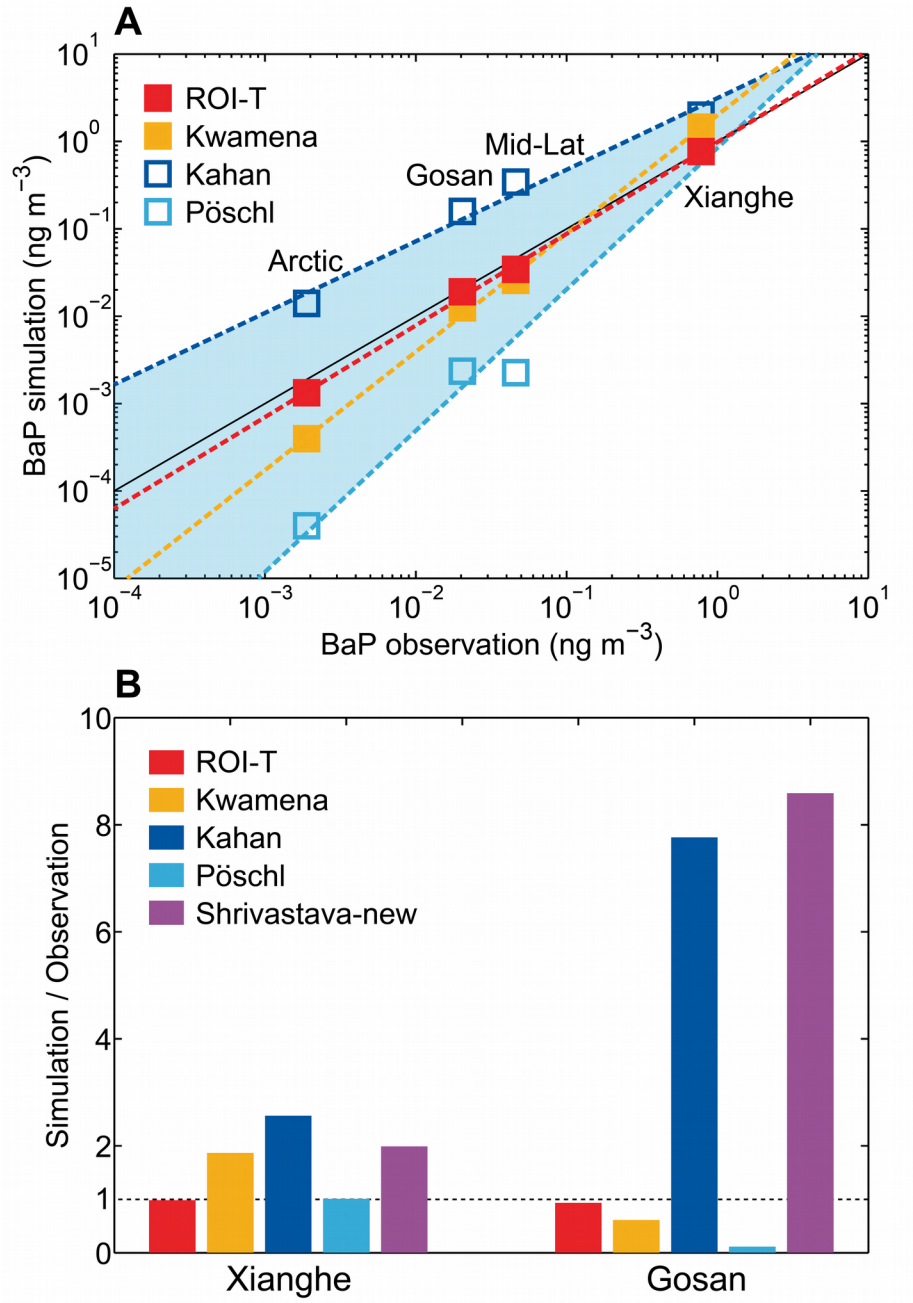

Fig. 2. Comparisons of the ROI-T scheme and previous laboratory derived schemes with observations. (**A**) Simulated concentrations of BaP (ng m^{-3}) by the ROI-T, Kwamena, Kahan and Pöschl schemes at the Xianghe site, the Gosan site, other mid-latitude sites, and the Arctic sites. The solid black line is 1:1 line of simulation and observation. The dashed lines are fitted by respective simulations. The shaded area is constrained by the Pöschl and the Kahan schemes. (**B**) The ratios of simulated and observed BaP concentrations with different schemes at the Xianghe site and the Gosan site.

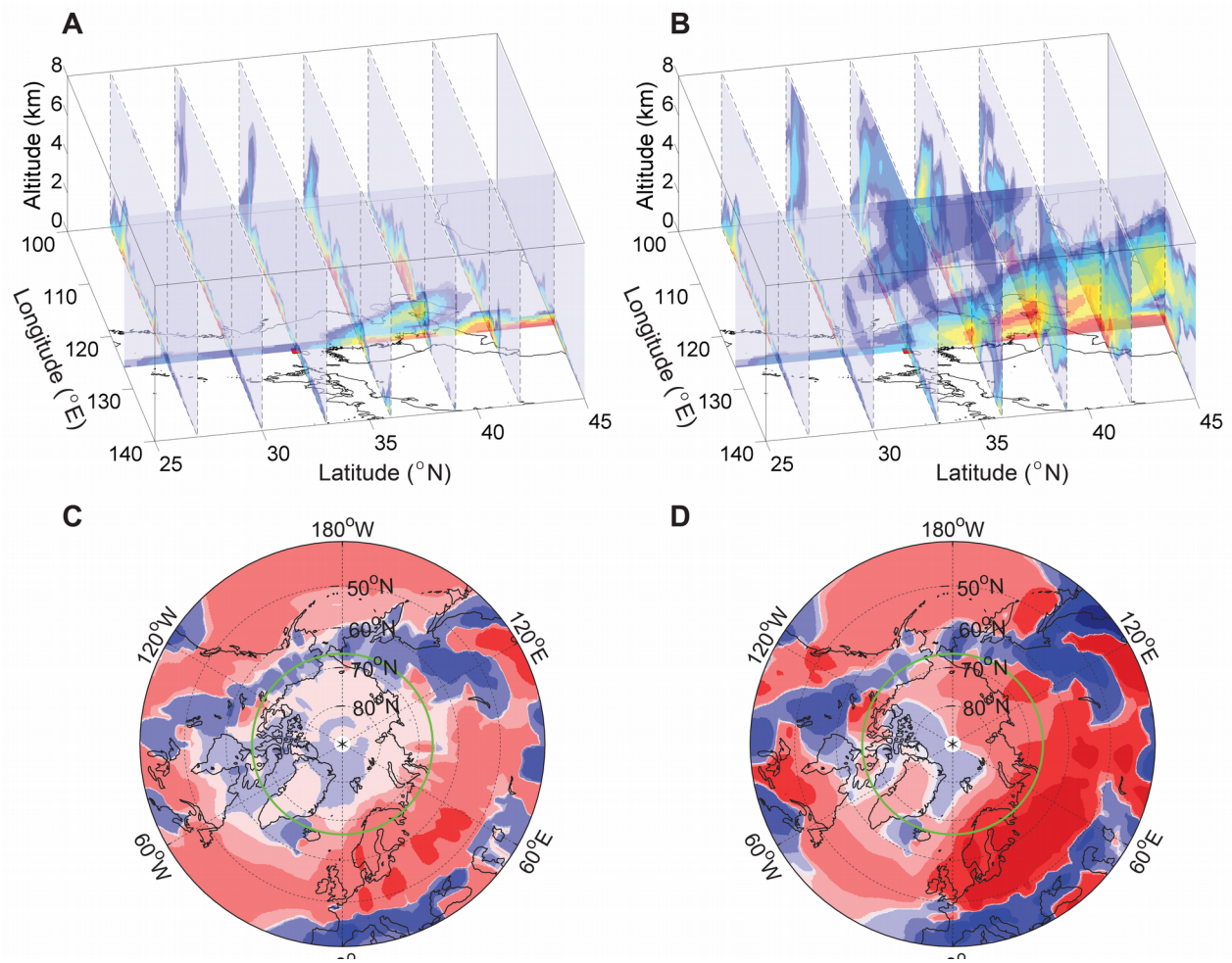

Fig. 3. Implications on the transport. Average concentrations of BaP (ng m^{-3}) in a strong East Asia outflow episode on 24 February 2003 are shown for the (**A**) Kwamena scheme and the (**B**) ROI-T scheme. Longitude cross section locates at 126º E. BaP net meridional flux (ng m^{-2} s^{-1}) averaged over years 2007–2009 are shown for the (**C**) Kwamena scheme and the (**D**) ROI-T scheme. Northward has Positive values (red) and southward has negative values (blue). Green circle marks the Arctic Circle at 66.56º N.

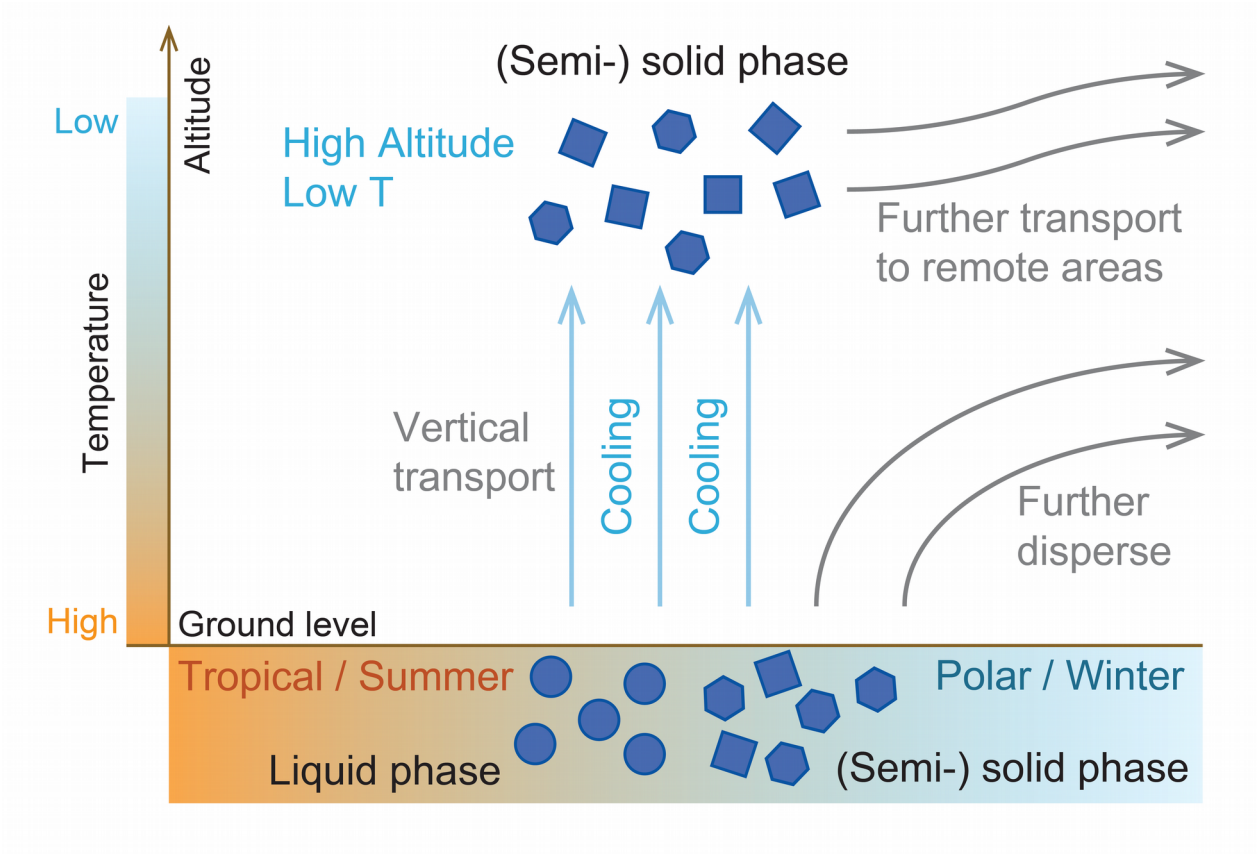

Fig. 4. Diagram of temperature/RH effects on BaP transport in ambient air. OA diffusivity and chemical reactivity are both reduced in response to changes in season (summer to winter), latitude (tropical to polar) and altitude (surface to high altitude), when OA phase state also changes from liquid to (semi-) solid phase. With a slower degradation rate and hence prolonged lifetime, BaP can be further dispersed and transported.